Inhibition of the Wnt/β-catenin signaling pathway and SOX9 by XAV939 did not alleviate inflammation in a dextran sulfate sodium-induced ulcerative colitis model

SHAO-JIE LIANG[1,2], KUN WANG[1], DA-BIN MAO[1], LI-WEI XIE[3] and DA-JIAN ZHU[1]

[1]Maternal and Children's Health Research Institute, Shunde Women and Children's Hospital, Guangdong Medical University, Foshan, Guangdong 528300, P.R. China; [2]The Marine Biomedical Research Institute of Guangdong Zhanjiang, Guangdong Medical University, Zhanjiang, Guangdong 524023, P.R. China; [3]State Key Laboratory of Applied Microbiology Southern China, Guangdong Provincial Key Laboratory of Microbial Culture Collection and Application, Guangdong Open Laboratory of Applied Microbiology, Institute of Microbiology, Guangdong Academy of Sciences, Guangzhou, Guangdong 510075, P.R. China

Received June 26, 2024; Accepted September 12, 2024

DOI: 10.3892/etm.2024.12774

Abstract. The Wnt/β-catenin signaling pathway has been reported to be hyperactivated during the pathogenesis of ulcerative colitis (UC). The present study aimed to explore the therapeutic efficacy of the Wnt/β-catenin signaling inhibitor XAV939 in mitigating UC symptoms. Utilizing a dextran sulfate sodium (DSS)-induced UC mouse model, the present study aimed to evaluate the impact of XAV939 on intestinal morphology through hematoxylin and eosin staining and to measure the expression levels of critical proteins in the Wnt/β-catenin signaling cascade. XAV939 did not exert a significant influence on the morphological features and inflammatory status of the intestinal epithelium. However, XAV939 was found to effectively suppress the Wnt/β-catenin signaling pathway and its downstream target SOX9. This suppression implied a reduction in the differentiation of intestinal stem cells into secretory cell progenitor cells. Additionally, XAV939 was ineffective at reversing the DSS-induced decrease in expression levels of Villin and peroxisome proliferator-activated receptor γ, which suggested that it did not facilitate the differentiation of intestinal absorptive cells. The present findings indicated that the Wnt/β-catenin signaling pathway may not be the predominant mechanism in the pathogenesis of DSS-induced UC.

Correspondence to: Professor Da-Jian Zhu, Maternal and Children's Health Research Institute, Shunde Women and Children's Hospital, Guangdong Medical University, 3 Baojian Road, Shunde, Foshan, Guangdong 528300, P.R. China
E-mail: zdj123zhudajian123@126.com

Professor Li-Wei Xie, State Key Laboratory of Applied Microbiology Southern China, Guangdong Provincial Key Laboratory of Microbial Culture Collection and Application, Guangdong Open Laboratory of Applied Microbiology, Institute of Microbiology, Guangdong Academy of Sciences, 100 Xianlie Middle Road, Guangzhou, Guangdong 510075, P.R. China
E-mail: xielw@gdim.cn

Key words: ulcerative colitis, XAV939, intestinal stem cell, Wnt/β-catenin, SOX9

Introduction

Ulcerative colitis (UC) is a chronic inflammatory bowel disease characterized by inflammation and ulcers in the lining of the colon and rectum, and the incidence rate of UC is steadily increasing globally, with the prevalence of UC estimated to be 5 million cases worldwide by 2023 (1). It typically affects the innermost lining of the colon and causes symptoms such as abdominal pain, diarrhea, rectal bleeding and weight loss (2). The etiology of this disease is believed to be multifaceted, with a growing emphasis on aberrant immune reactions, gut dysbiosis, genetic predisposition and environmental influences (3). Treatment of UC usually involves medication to reduce inflammation, manage symptoms and maintain remission (3). Although sulfasalazine, 5-aminosalicylates, corticosteroids, thiopurines and methotrexate have traditionally served as the primary and initial treatment options for patients with UC, treatment with biological agents is now advisable for those experiencing moderate to severe symptoms (4,5). In severe cases, surgery to remove the affected portion of the colon is necessary (6). However, none of the currently available treatment methods are deemed entirely satisfactory due to the side effects caused by long-term medication use and the high recurrence rate, and the identification of the ideal treatment remains elusive.

Multiple studies have reported that UC activates the colonic Wnt/β-catenin signaling pathway, which is intricately linked to the upregulation of inflammatory cytokines (7-9). Furthermore, chronic inflammation in UC increases the risk of developing colorectal cancer, which is closely related to the excessive activation of the Wnt/β-catenin signaling pathway (10,11). Furthermore, inhibiting the Wnt/β-catenin signaling pathway has been reported to be advantageous in the treatment of UC (12,13). Among the inhibitors of the Wnt/β-catenin

signaling pathway, XAV939 exhibits suppressive effects on the inflammatory response triggered by lipopolysaccharide (LPS) (14,15). Consequently, the utilization of XAV939 to block the Wnt/β-catenin signaling pathway presents a feasible approach to effectively manage the inflammation associated with UC.

The Wnt/β-catenin signaling pathway serves a critical role in regulating the differentiation of intestinal stem cells (ISCs) (16). By modulating the expression of Wnt/β-catenin and its downstream effector SOX9, it regulates the process of ISC differentiation into secretory cell progenitor cells (17). It is suggested that there is upregulated activity of the Wnt/β-catenin signaling pathway in UC and this is believed to contribute to the abnormal expansion of ISCs observed in UC (18). There is an increased tendency for ISCs to differentiate into secretory progenitor cells in the colon of patients with UC (19). However, this disruption hinders the normal healing process of the intestinal mucosa and compromises the functionality of the intestinal barrier and its absorption capabilities. Understanding the mechanisms underlying ISCs and their potential as therapeutic targets could provide invaluable insights and novel approaches for the management of UC.

The present study aimed to validate the therapeutic effects of the Wnt/β-catenin inhibitor XAV939 on dextran sulfate sodium (DSS)-induced UC and to assess its impact on ISC differentiation.

Materials and methods

Animals. All animal procedures were performed in accordance with the Guidelines for Care and Use of Laboratory Animals of Guangdong Medical University and the experiments were approved by the Ethics Committee of Shunde Women and Children's Hospital of Guangdong Medical University (approval no. 2023054; Foshan, China).

Animal welfare. An enriched environment, nutritious diet and humane handling were provided to the animals. All the mice were provided by the Guangdong Medical Laboratory Animal Center and housed in a specific pathogen-free facility (temperature, 23±1˚C; 12/12 h light/dark cycle; humidity, 50-60%). A single mouse was used as the experimental unit and the placement of cages was random throughout the space used. Measures were taken to ensure the welfare of the animals and to minimize discomfort for all animals involved in the present study. Animals were fed daily with a fresh diet to maintain body weight and normal growth. All mice were allowed *ad libitum* access to food and water. The criteria used to determine when animals should be euthanized included, but were not limited to, loss of body weight of 20% compared with the body weight before the study began, severe behavioral abnormalities or physiological distress. In the present study, a maximum weight loss of 19.78% was observed. The mice were euthanized by intraperitoneal injection of 100 mg/kg pentobarbital sodium. Death was verified by checking for the cessation of the heartbeat and pupil dilation.

Experimental design. The experiments were performed during the 12 h light cycle. For RNA-sequencing (RNA-seq) experiment, a total of 6 healthy male C57BL/6 mice (body weight, 18-22 g; age, 8 weeks) were randomly divided into two groups (n=3/group). The control group received distilled water, while the treatment group received 3.5% DSS for 7 days. For the intervention study, a total of 18 healthy male C57BL/6 mice (body weight, 18-22 g; age, 8 weeks) were randomly divided into three groups (n=6/group): i) Control group; ii) DSS group (3.5% DSS) and iii) DSS + XAV939 group [DSS + XAV, 3.5% DSS + 10 mg/kg body weight (BW) XAV939]. In our previous study, we did not observe colitis-related changes when utilizing low concentrations of DSS to induce the UC model (unpublished data). Subsequently, findings from other literature were cross-referenced and the experimental model of DSS administration was adjusted accordingly (20,21). Throughout the experiment, there were no instances of animal mortality observed prior to its conclusion. The dose of XAV939 was determined in accordance with the report conducted by Distler *et al* (22). DSS was dissolved in drinking water and XAV939 was dissolved in DMSO (≥99.7%; cat. no. D2650; Sigma-Aldrich, Inc.) and 0.4 ml was administered by intraperitoneal injection for 7 days. The control and DSS groups were injected with 0.4 ml PBS mixed with the same concentration of DMSO (Fig. S1). All mice were euthanized and the entire colon was collected. The length of colons, average daily weight gain and weight of the colon per unit length were examined to measure the treatment outcome. DSS was purchased from Dalian Meilun Biology Technology Co., Ltd. and XAV939 was purchased from MedChemExpress (cat. no. HY-15147).

Analysis of colonic crypt RNA-seq transcriptomic data using bioinformatics. RNA extraction and purification from colonic crypts were carried out in accordance with the manufacturer's instructions (cat. no. 74104; Qiagen GmbH). The total RNA of colonic crypts from the control and DSS groups were sequenced by Guangdong Magigene Biotechnology Co., Ltd. The Agilent 4200 Bioanalyzer (Agilent Technologies, Inc.) was used for quality control of samples. All samples had RNA integrity numbers >8. Subsequently, 150 bp paired-end reads were generated using the Illumina NextSeq sequencing platform (Illumina, Inc.).

Raw reads were first trimmed with Trimmomatic (version 0.36; http://www.usadellab.org/cms/index.php?page=trimmomatic) to acquire the clean reads, which were then mapped to National Center for Biotechnology Information Rfam databases (version 14.10; https://rfam.org) and the rRNA sequences removed using Bowtie2 (version 2.33; https://github.com/BenLangmead/bowtie2). The reads were mapped to the mouse reference genome (Mus_musculus_GCF_000001635.27) using Hisat2 (version 2.1.0; https://github.com/infphilo/hisat2) (23,24). HTSeq-count (version 0.9.1; http://htseq.readthedocs.io/en/release_0.9.1/) was used to obtain the read count and function information of each gene. The count tables were normalized based on their library size using trimmed mean of M-values normalization implemented in R/Bioconductor EdgeR (version 3.34.0; http://www.bioconductor.org/packages/release/bioc/html/edgeR.html) (25,26). Normalized read counts were fitted to a negative binomial distribution with a quasi-likelihood F-test. Principal component analysis (PCA; https://www.r-project.org) was performed for the regularized log transform of the normalized counts using plotPCA tools with default parameters (27,28). Differential

Table I. Primer sequences used for reverse transcription-quantitative PCR.

Gene	Sequence (5'-3')
TNF-α	F: CTGGGACAGTGACCTGGACT
	R: GCACCTCAGGGAAGAGTCTG
IL-1β	F: TTCAGGCAGGCAGTATCACTCATT
	R: TTGTTCATCTCGGAGCCTGTAGTG
SOX9	F: GGGGCTTGTCTCCTTCAGAG
	R: TGGTAATGAGTCATACACAGTAC
Villin	F: TATCATCGTGGTGAAGCAGGGACA
	R: GGGCTCATAACCTCGTCAGCAATCT
β-catenin	F: TGTACTGTTCTACGCCATCACGA
	R: CTAGAGCAGACAGACAGCACCTTC
Peroxisome proliferator activated receptor-γ	F: TTTTCAAGGGTGCCAGTTTCG
	R: GGGCTTCCGCAGGCTTTT
GAPDH	F: TGTTTGTGATGGGTGTGAACC
	R: GCAGTGATGGCATGGACTGTG

F, forward; R, reverse.

gene expression analysis was further carried out using EdgeR. The log2 fold change <-1 or >1 and a P-value <0.05 were used to examine differentially expressed genes (DEGs). The Kyoto Encyclopedia of Genes and Genomes (KEGG) and Gene Ontology (GO) analysis was also used to calculate DEG enrichment, which could be used to obtain information on the fold changes of expressed genes at the molecular level. To determine the metabolic and signaling pathways, the DEGs at various KEGG pathway levels were counted. The log2 fold change <-1 or >1 and a P-value <0.05 were used to examine differentially for KEGG and GO analyses.

Histological examination of tissues and immunohistochemical (IHC) staining. The colons were collected and fixed in 4% paraformaldehyde, with fixation typically conducted at room temperature (20-25˚C) for 24 h. Following fixation, the colons were paraffin embedded and sectioned at a thickness of 5 μm for histological analysis and IHC. Hematoxylin and eosin (H&E) staining was used to assess morphological changes in the intestine, and was imaged (Evos XL Core; Thermo Fisher Scientific, Inc.). Tissue sections were dewaxed and rehydrated, and then stained with hematoxylin for 5 min to highlight nuclear structures. Next, the sections were rinsed and counterstained with eosin for 1 min to color the cytoplasm and extracellular matrix. The staining was carried out at room temperature (20-25˚C). Finally, the sections were dehydrated, cleared and mounted onto slides for microscopic examination. Antigen repair was performed on paraffin sections using EDTA antigen repair solution (cat. no. ZLI-9067; ZSBG-BIO) in boiling water for 10 min, then blocked with fetal bovine serum at room temperature for 1 h. IHC staining for IL-1β (cat. no. ab234437; Abcam), SOX9 (cat. no. ab185230; Abcam), β-catenin (cat. no. R22820; Zenbio), Villin (cat. no. SC58897; Santa Cruz Biotechnology, Inc.) and PPAR-γ (cat. no. 16643-1-AP; Wuhan Sanying Biotechnology) was performed. The dilution ratio of primary antibody was 1:100, and the incubations for primary antibodies were conducted at 4˚C for a duration of 16 h. The samples were then washed with PBS three times and incubated with Cy3 (cat. no. K1209; APeXBIO Technology LLC) and FITC (cat. no. IF-0091; Beijing Dingguo Changsheng Biotechnology Co., Ltd.)-labeled fluorescent secondary antibodies (1:500) for 1 h at room temperature. The dilutions for all antibodies used were prepared using a universal antibody dilution buffer (cat. no. WB500D; New Cell & Molecular Biotech Co., Ltd.). The nuclei were stained with DAPI (cat. no. C55-141215; Biosharp Life Sciences) (1:1,000 dilution) for 10 min at room temperature. Images were obtained using a confocal microscope (LSM 900; Carl Zeiss AG). The fluorescence signal intensity was measured with ImageJ software (ImageJ2x 2.1.4.7; National Institutes of Health), and the minimum value in the control group was set to 1.

RNA extraction and reverse transcription-quantitative PCR (RT-qPCR). The RNA was extracted from cultured intestinal organoids. RNA extraction was performed was performed using a FastPure cell/tissue RNA isolation kit V2 (cat. no. RC112-01; Vazyme Biotech Co., Ltd.), according to the manufacturer's instructions. The reverse transcription process followed RNA extraction using a reverse transcription kit (HiScript II Q RT SuperMix for qPCR; cat. no. R222-01; Vazyme Biotech Co., Ltd.), which involved incubating the reaction mixture at 50˚C for 15 min and subsequently at 85˚C for 30 sec. The primers were purchased from Sangon Biotech Co., Ltd. (Table I). qPCR of TNF-α, IL-1β, Villin, peroxisome proliferator-activated receptor γ (PPAR-γ), SOX9 and β-catenin was performed. To normalize gene expression, a GAPDH endogenous control was used. The ChamQ Universal SYBR qPCR Master Mix (cat. no. Q711-02; Vazyme Biotech Co., Ltd.) and qPCR was employed to verify the mRNA expression using a platform from Applied Biosystems; Thermo Fisher Scientific, Inc. The reaction conditions set were as follows: An initial denaturation

at 94˚C for 5 min; followed by 36 cycles of (denaturation at 94˚C for 30 sec, annealing at 60˚C for 30 sec, and extension at 72˚C for 30 sec); a final extension at 72˚C for 5 min; and a subsequent incubation at 60˚C for 30 sec followed by 95˚C for 30 sec. PCR amplification was analyzed using the comparative $2^{-\Delta\Delta Cq}$ method (29).

Crypt culture and treatment of intestinal organoids. The crypts were isolated by taking ~5 centimeters of colon and splitting it longitudinally. The intestinal contents were then cleaned using PBS and transferred to a 15 ml centrifuge tube and 5 ml of PBS was added. After gently shaking by hand for 5 min, the solution was replaced with fresh PBS and the shaking process was repeated six times. The colon segments were then cut into 1 cm pieces. The PBS was discarded, and a solution containing 30 mmol/l EDTA-2Na and 1.5 mmol/l dithiothreitol in PBS was added. The solution was gently shaken by hand for 5 min, then the separation solution was replaced and the shaking process was repeated once. Fresh PBS was added, and the suspension was observed for crypt units and debris impurities. When there were more crypt units and less debris impurities, fresh PBS was added and the sample was shaken vigorously by hand for 1 min, incubated on ice for 5 min and the crypts were collected. The quality of the isolated crypts served a crucial role in the success of organoid culture. The crypts obtained exhibited intact structures and a high purity (>90% of them retained the intact structure of the crypt base), ensuring the quality of the resulting organoids (Fig. S2). Crypts were embedded in Matrigel and cultured using a mouse colonic organoid kit (cat. no. K2204-MC; Biogenous), and the seeding density of the crypts was 5/1 μl of matrix gel, with 8 μl per well (40 crypts in total). The organoid was cultured in a CO_2 incubator at 37˚C. At 24 h post-crypt seeding, a gradual transformation of the crypts into rounded and transparent structures was observed using a Evos XL Core microscope (Thermo Fisher Scientific, Inc.), which is a characteristic feature of organoid formation. The intestinal organoid was induced with TNF-α to establish an inflammatory model. TNF-α and XAV939 treatment was performed after 48 h of seeding, and the sample in each well served as a replicate and was collected after 24 h of treatment. The intestinal organoids were divided into three groups: i) Control group; ii) TNF-α group treated with 100 ng/ml TNF-α (cat. no. 10602-R101-F; Sino Biological, Inc.); and iii) TNF-α+XAV939 group treated with 100 ng/ml TNF-α and 10 μM XAV939. The dose of XAV939 used was determined in accordance with the previous report by Liang *et al* (30). The organoid formation efficiency was calculated by dividing the number of colonies formed by the number of crypts seeded and expressing this as a percentage. The surface area was measured using ImageJ software (ImageJ2X 2.1.4.7, National Institutes of Health).

Western blotting. The colon samples collected from various groups in the XAV939 experiment were used to prepare protein samples. The colon was lysed by RIPA (cat. no. WB3100; New Cell & Molecular Biotech Co., Ltd.) and prepared into protein samples of the same concentration by the BCA kit (cat. no. P0011; Beyotime Institute of Biotechnology). The sample loading amount per lane was 10 μg. Protein samples were separated on 10% SDS-PAGE gels and transferred to PVDF membranes. The membranes were blocked with 5% bovine serum albumin at room temperature for 1 h. The membranes were incubated with primary antibodies at 4˚C for 12-16 h. The selection and use of these primary antibodies were consistent with the description for IHC: IL-1β (cat. no. ab234437; Abcam), SOX9 (cat. no. ab185230; Abcam), β-catenin (cat. no. R22820; Zenbio), Villin (cat. no. SC58897; Santa Cruz Biotechnology, Inc.) and PPAR-γ (cat. no. 16643-1-AP; Wuhan Sanying Biotechnology). The dilution ratio of primary antibody was 1:1,000, and the dilutions for all antibodies used were prepared using a universal antibody dilution buffer (cat. no. WB500D; New Cell & Molecular Biotech Co., Ltd.). Samples were washed using TBS with Tween-20 (0.1%) three times and incubated with a HRP-goat anti-rabbit secondary antibody (cat. no. RGAR001; Wuhan Sanying Biotechnology) and a HRP-goat anti-mouse secondary antibody (cat. no. SA00001-1; Wuhan Sanying Biotechnology) for 1 h at room temperature. The enhanced chemiluminescence (KF8001; Affinity Biosciences) signals were scanned using a ChemiDOC XRS+ (Bio-Rad Laboratories, Inc.), and the band densities were analyzed using ImageJ software.

Statistical analysis. GraphPad Prism (version 8.0; Dotmatics) software was utilized for statistical analysis. All data were presented as the mean ± SEM. Multiple comparisons were performed using a one-way ANOVA and Tukey's post hoc test. $P<0.05$ was considered to indicate a statistically significant difference.

Results

RNA-seq demonstrated changes in ISC differentiation in the UC model. The colonic crypts were isolated for RNA-seq (Fig. 1A). PCA results showed a significant difference between the control group compared with the DSS group (Fig. 1B). A total of 212 genes were upregulated and 315 genes were downregulated after DSS treatment (Fig. 1C). KEGG analysis demonstrated that DSS treatment resulted in the differentially expressed genes related to various types of metabolic processes (Fig. 1D). Additionally, KEGG analysis showed significant changes in inflammatory cytokine receptor interactions and MAPK signaling pathways (Fig. 1E). The DSS group showed significant down-regulation of intestinal goblet cell and enterocyte marker genes, and a significant increase in secreting cell progenitor marker genes, which indicated a potential disorder in ISC differentiation (Fig. 1F). Furthermore, DSS significantly altered the gene abundance of inflammatory factors and other niche factors, which is crucial for the microenvironmental homeostasis of ISCs (Fig. 1F).

Effect of XAV939 on the DSS-induced UC model in mice. To confirm the therapeutic effect of XAV939 on DSS-induced UC in mice, the length of the colon was measured (Fig. 2A). Compared with the control group, DSS caused significant shortening of the colon (Fig. 2B, $P<0.01$) and a significant reduction in average daily weight gain (Fig. 2C, $P<0.01$). However, the results showed that treatment with XAV939 had no significant effect on the colon length compared with the DSS group (Fig. 2B, $P=0.95$). Additionally, XAV939 did not significantly improve the average daily weight gain compared

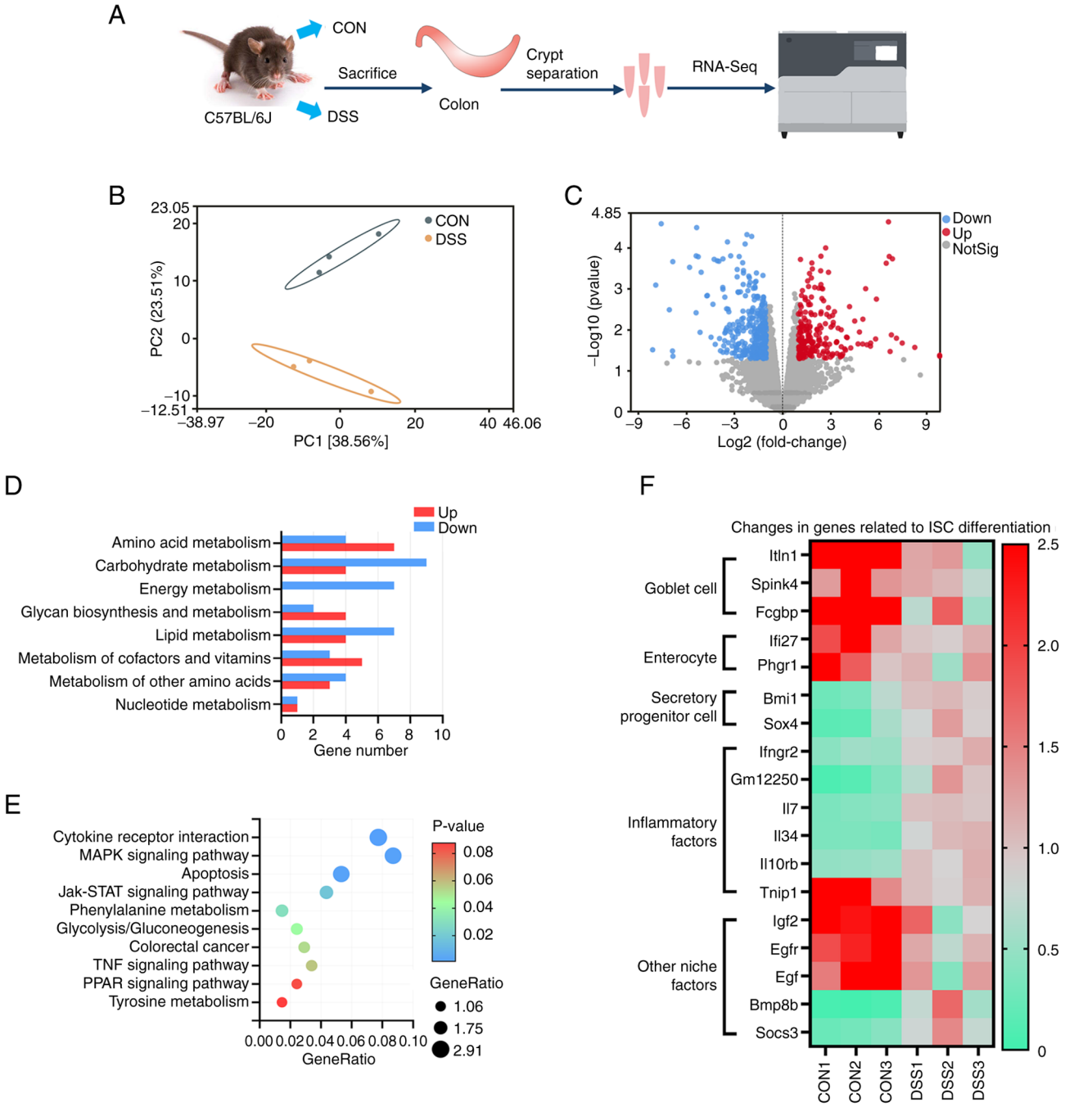

Figure 1. Results of RNA-seq analysis. (A) Experimental setup and procedures for RNA-seq. (B) Principal component analysis comparing the control and DSS groups. (C) Statistics summarizing the expression differences between control and DSS samples. (D) Kyoto Encyclopedia of Genes and Genomes pathway enrichment analysis to identify significantly altered genes related to various types of metabolic processes. (E) Kyoto Encyclopedia of Genes and Genomes pathway enrichment analysis to identify altered signaling pathways. (F) Changes in the expression of genes related to secretory progenitor cells, enterocytes and goblet cells, inflammatory factors and other niche factors were examined. DSS, dextransulfate sodium; RNA-seq, RNA-sequencing; CON, control; NotSig, not significant.

with the DSS group (Fig. 2C, P=0.98). XAV939 treatment caused an increase in the weight of the colon per unit length compared with the DSS group (Fig. 2D, P=0.09), which indicated that the colon injury treated by DSS was not improved. Therefore, XAV939 may not be beneficial in mitigating the colonic changes associated with DSS-induced UC in mice.

XAV939 did not improve the DSS-induced inflammation. The results of H&E staining showed that XAV939 treatment caused no significant difference in colonic epithelial structure and inflammatory infiltration compared with the DSS group (Fig. 3A). The increase in crypt depth, which can be considered a marker of intestinal damage, was significantly more pronounced after XAV939 treatment compared with the DSS group, which indicated that there was improvement in colon injury (Fig. 3B, P<0.01). Furthermore, the results of western blotting demonstrated that, compared with the control group, the DSS group exhibited a significant increase in IL-1β protein expression levels (Fig. 3C and D, P<0.05). The non-specific bands in the GAPDH blot may have been due to the high

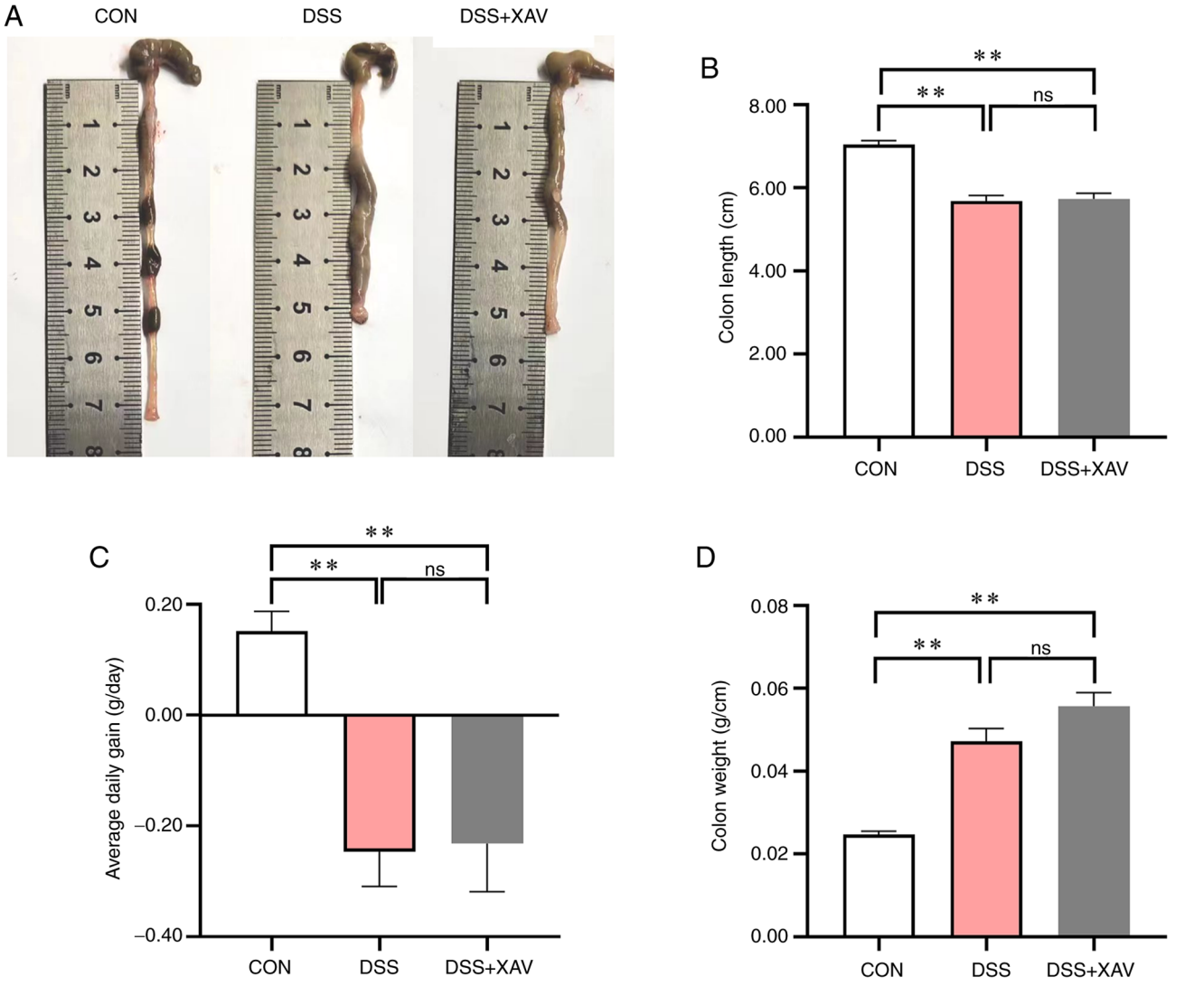

Figure 2. Effect of XAV on the DSS-induced ulcerative colitis model in mice. (A and B) Measurement of the lengths of the colons. (C) Average daily weight gain. (D) Weight of the colon per unit length. Data are presented as the mean ± SEM (n=6). **P<0.01. Ns, not significant; DSS, dextran sulfate sodium; CON, control; XAV, XAV939.

concentration of antibodies used. The results of IHC also demonstrated that the DSS induced a significant increase in the expression level of IL-1β (Fig. 3E and F, P<0.05). Notably, supplementation with XAV939 did not lead to significant changes in IL-1β protein expression levels (Fig. 3D, P=0.38; Fig. 3F, P=0.09). These findings collectively suggested that XAV939 had no beneficial effect on DSS-induced colon injury and inflammation.

Effect of XAV939 on the mouse intestinal organoid treated with TNF-α. Due to the severe damage caused by DSS to the intestinal epithelium and the key role of ISCs in promoting the repair process of the epithelium, the intestinal organoid model was used to verify the anti-inflammatory effect of XAV939 (Fig. 4A). These results demonstrated that XAV939 significantly reduced the forming efficiency of organoids compared with the TNF-α group (Fig. 4B, P<0.01), and significantly alleviated the TNF-α-induced increase in organoid area (Fig. 4C, P<0.01). TNF-α did not affect the forming efficiency of the organoid, but the stimulation was successful because TNF-α treatment led to a significant increase in TNF-α (Fig. 4D, P<0.01) expression level, and an increase in IL-1β (Fig. 4E, P=0.81) expression level. Nevertheless, the addition of XAV939 did not significantly reduce the expression levels of IL-1β and TNF-α induced by TNF-α treatment (Fig. 4D, P=0.47). Notably, the addition of XAV939 contributed to an increase in IL-1β expression levels (Fig. 4E, P<0.01), which indicated that XAV939 did not significantly relieve inflammation.

XAV939 reduced the expression levels of β-catenin and SOX9. As the differentiation of ISCs is regulated by the Wnt/β-catenin signaling pathway, the protein expression levels of β-catenin and its downstream target SOX9 were examined (Fig. 5A). DSS significantly increased β-catenin (Fig. 5B, P<0.01) and SOX9 (Fig. 5B, P<0.05) protein expression levels, while XAV939 significantly reduced the protein expression levels of β-catenin (Fig. 5B, P<0.05) and SOX9 (Fig. 5B, P<0.01) compared with the DSS group. Simultaneously, β-catenin and SOX9 protein expression was determined by

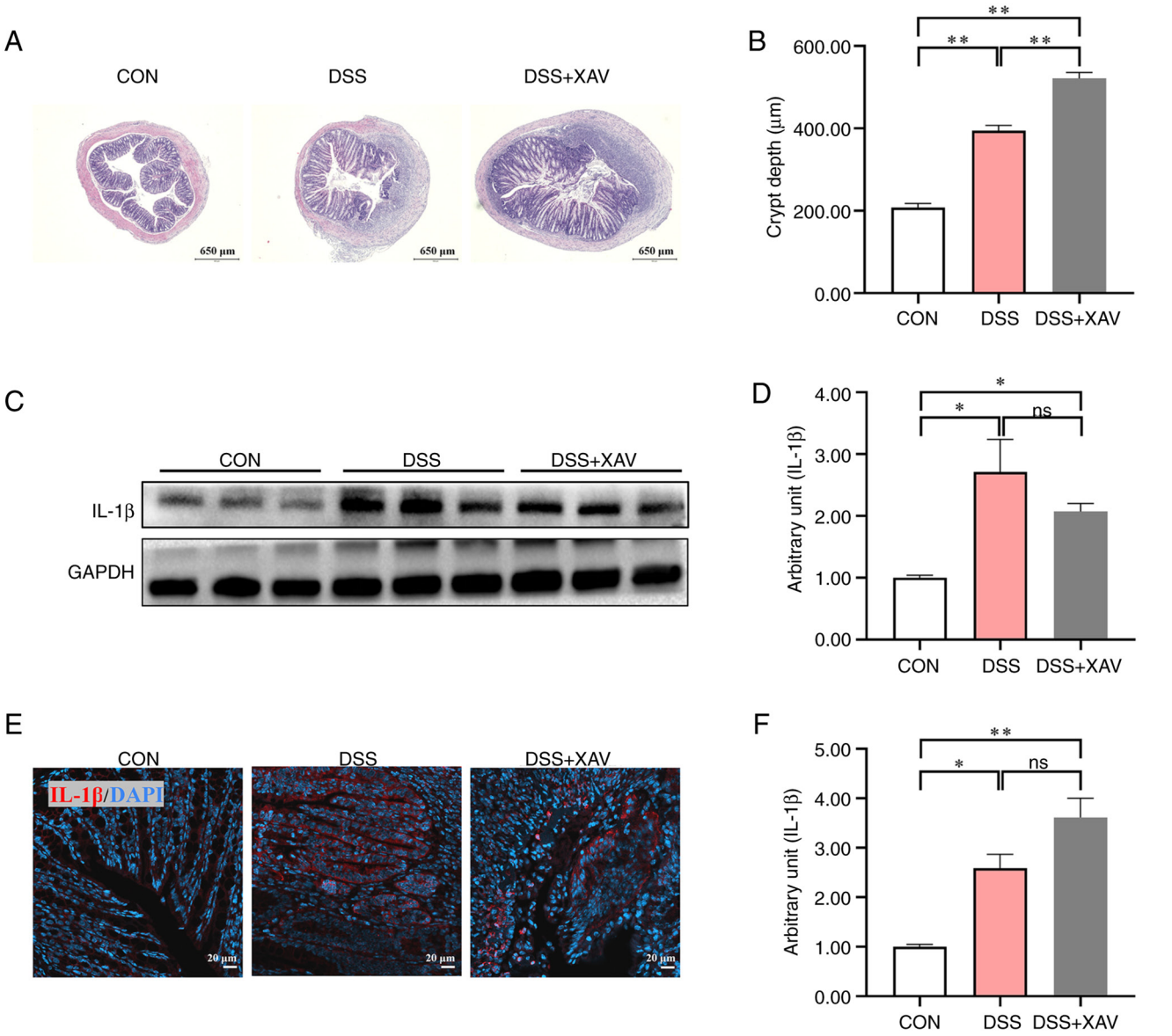

Figure 3. XAV did not alleviate DSS-induced inflammation. (A) Hematoxylin and eosin staining of the colon, showing the histopathological features (scale bar, 650 μm). (B) Crypt depth of the colon. (C and D) Expression levels of IL-1β in the colon. (E) Images of immunohistochemistry staining with IL-1β antibodies of the colon, demonstrating the localization of IL-1β expression (scale bar, 20 μm). (F) Fluorescence intensity of IL-1β. Data are presented as the mean ± SEM (n=3). *P<0.05, **P<0.01. Ns, not significant; DSS, dextran sulfate sodium; CON, control; XAV, XAV939.

IHC (Fig. 5C). DSS significantly increased the fluorescence intensity of β-catenin (Fig. 5D, P<0.05) and SOX9 (Fig. 5D, P<0.01), while XAV939 significantly reduced the fluorescence intensity of β-catenin (Fig. 5D, P<0.05) and SOX9 (Fig. 5D, P<0.01). In the intestinal organoid experiment, XAV939 treatment significantly reduced the TNF-α-induced increase in the expression levels of β-catenin (Fig. 5E, P<0.05) and SOX9 (Fig. 5E, P<0.01). These results indicated that XAV939 could reverse the excessive activation of Wnt/β-catenin induced by DSS and TNF-α.

XAV939 failed to reverse the reduction of PPAR-γ and Villin. Previous studies have suggested that the PPAR-γ signaling pathway serves a role in enterocyte differentiation, and Villin serves as a marker for enterocytes in the intestine (31,32). To further investigate the regulatory effect of XAV939 on enterocyte differentiation, western blotting was used to assess the protein expression levels of PPAR-γ and Villin (Fig. 6A). The results demonstrated that DSS treatment led to decreased protein expression levels of PPAR-γ (Fig. 6B, P<0.01) and Villin (Fig. 6B, P<0.05). However, XAV939 did not significantly reverse this decreased expression (Fig. 6B). Simultaneously, PPAR-γ and Villin protein expression was determined by IHC (Fig. 6C). DSS significantly decreased the fluorescence intensity of PPAR-γ (Fig. 6D, P<0.01) and Villin (Fig. 6D, P<0.05), while XAV939 did not significantly reverse the reduction of the fluorescence intensity of PPAR-γ (Fig. 6D, P=0.31) and Villin (Fig. 6D, P=0.99). In the intestinal organoid model, XAV939 significantly reduced the expression levels of PPAR-γ (Fig. 6E, P<0.01) and Villin (Fig. 6E, P<0.01) compared with the TNF-α group, which indicated that the organoid was more sensitive to the inhibitory effects of XAV939 compared with the ISC *in vivo*.

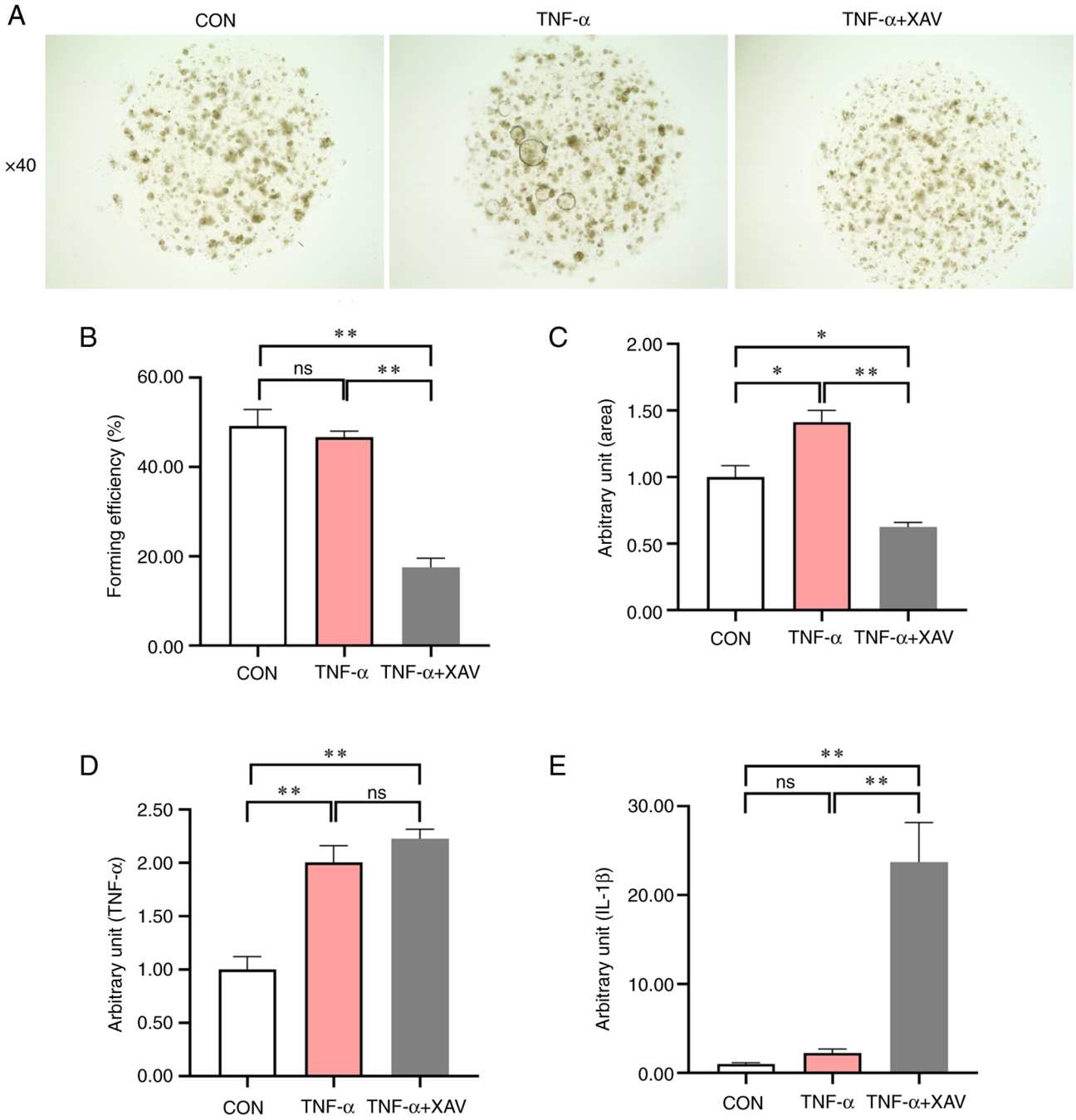

Figure 4. Effect of XAV on the mouse intestinal organoid treated with TNF-α. (A) Images of intestinal organoids expanded from crypts. Magnification, x40. (B) Formation efficiency of the intestinal organoids. (C) Surface area measurement of the intestinal organoids. (D and E) mRNA expression levels of TNF-α and IL-1β in the intestinal organoids. Data are presented as the mean ± SEM (n=4). *P<0.05, **P<0.01. CON, control; XAV, XAV939; ns, not significant.

Discussion

The present study provided insights into the effect of XAV939 on Wnt/β-catenin signaling in a mouse model of DSS-induced UC and suggested its potential association with the differentiation of secretory progenitor cells. Nevertheless, the present findings showed that XAV939 did not increase the length of the colon, enhance epithelial structure or reduce inflammatory cytokines. These results indicated that XAV939 may not be efficient in the treatment of UC. The present study further demonstrated that XAV939 effectively suppressed SOX9, a downstream target of the Wnt/β-catenin signaling pathway, in DSS-induced UC. SOX9 serves a pivotal role in regulating the differentiation of ISCs into secretory progenitor cells (33). Therefore, XAV939 may show potential to reverse the excessive differentiation of secretory progenitor cells in the DSS-induced UC mouse model. However, the present study demonstrated that the use of XAV939 did not mitigate inflammation. XAV939 regulated the differentiation of secretory cell progenitor cells via the Wnt/β-catenin signaling pathway. Unraveling the complex mechanisms underlying ISC differentiation and its dysregulation in UC is crucial for developing effective therapeutic strategies.

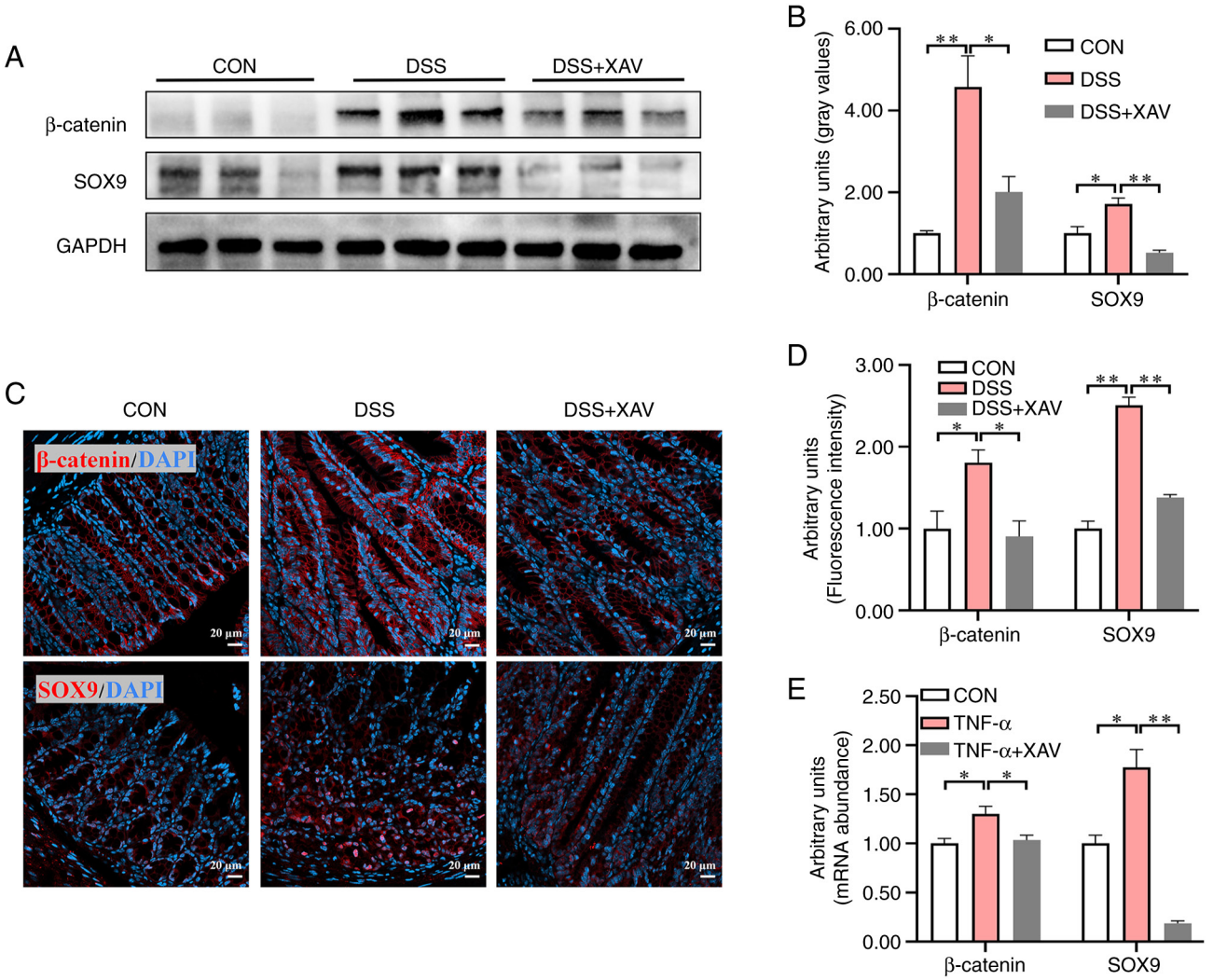

Figure 5. XAV reduced the expression levels of β-catenin and SOX9. (A and B) Protein expression levels of β-catenin and SOX9 in the colon were measured, demonstrating a decrease following XAV treatment. (C) Images of immunohistochemistry staining with β-catenin and SOX9 antibodies in the colon demonstrated the localization of these proteins (scale bar, 20 μm). (D) Fluorescence intensity of β-catenin and SOX9, reflecting their protein expression levels, was quantified. (E) mRNA expression levels of β-catenin and SOX9 in intestinal organoids was assayed. Data are presented as the mean ± SEM (n=3). *P<0.05, **P<0.01. CON, control; XAV, XAV939; DSS, dextran sulfate sodium.

The mechanism by which DSS induces UC is not fully understood, but it may include several aspects, such as damaging colonic epithelial cells, activating immune inflammatory responses and disrupting the intestinal flora balance (34). XAV939 may exert therapeutic effects by regulating ISC differentiation and inhibiting inflammatory responses. However, the present study demonstrated that XAV939 did not exert a significant inhibitory effect on the inflammatory response induced by TNF-α, therefore, it was ineffective at suppressing the inflammatory storm caused by DSS. In the context of UC treatment, controlling inflammation is crucial for restoring the intestinal epithelium. The purpose of using XAV939 was to affect the Wnt/β-catenin signaling pathway and to simultaneously modulate the inflammatory response. A previous study reported that XAV939 exhibits suppressive effects on the inflammatory response induced by LPS (35). However, in the present study, XAV939 treatment did not lead to a decrease in the expression levels of inflammatory cytokines in the TNF-α-induced intestinal organoid model. This may be due to LPS and TNF-α inducing inflammation through distinct molecular mechanisms. LPS primarily acts through Toll-like receptor 4 (TLR4), while TNF-α signals through the tumor necrosis factor receptor superfamily (36,37). This suggests that the anti-inflammatory effects of XAV939 are mechanism-specific and may not be broadly applicable to all inflammatory stimuli. Additionally, the TLR4 and NF-κB signaling pathways serve crucial roles in the pathogenesis of UC. XAV939 can inhibit the activity of TLR4, which may be achieved by blocking the binding of TLR4 to its ligand or interfering with downstream signaling molecules of TLR4 (38). XAV939 does not have a direct inhibitory effect on NF-κB (39). As the activation of NF-κB is also regulated by other signaling pathways, the inhibitory effect of XAV939 on TLR4 may not be sufficient to completely block the regulatory effects of these signaling pathways on the inflammatory response, which results in its inability to effectively inhibit inflammation caused by DSS. The Wnt/β-catenin signaling pathway exhibits both stimulatory and inhibitory effects on NF-κB-mediated inflammation, and the underlying molecular mechanisms involved are complex

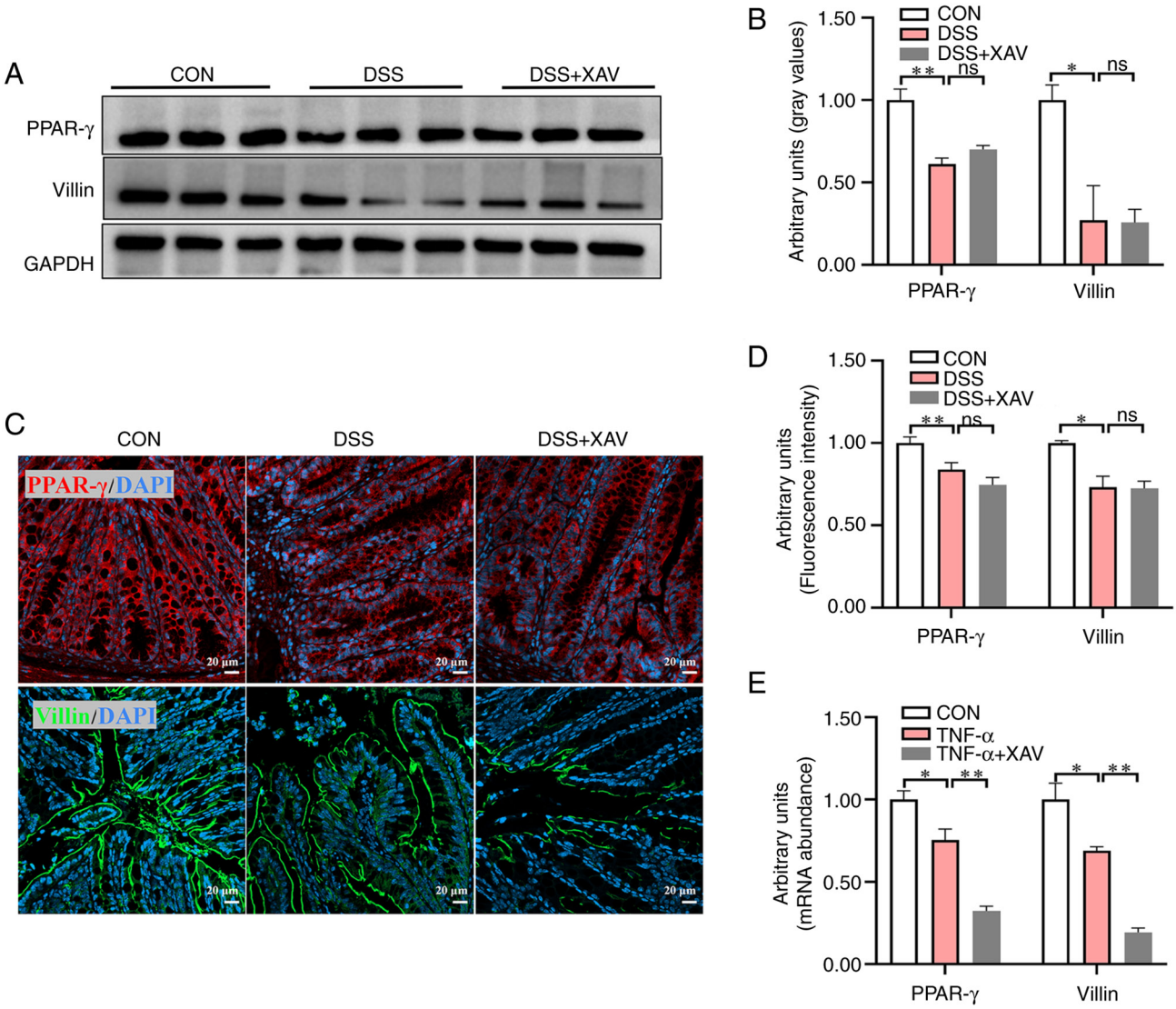

Figure 6. XAV failed to reverse or ameliorate the DSS-induced reduction of PPAR-γ and Villin. (A and B) Protein expression levels of PPAR-γ and Villin in the colon were measured, demonstrating a reduction in their levels following DSS treatment. (C) Images of immunohistochemistry staining with PPAR-γ and Villin antibodies in the colon demonstrated the localization and expression patterns of these proteins (scale bar, 20 μm). (D) Fluorescence intensity of PPAR-γ and Villin. (E) mRNA expression levels of PPAR-γ and Villin in intestinal organoids was assayed. Data are presented as the mean ± SEM (n=3). *P<0.05, **P<0.01. DSS, dextran sulfate sodium; PPAR-γ, peroxisome proliferator-activated receptor γ; CON, control; XAV, XAV939; DSS, dextran sulfate sodium; ns, not significant.

and multifaceted (40,41). Notably, the impact of β-catenin on NF-κB may vary depending on the specific genetic context or cell type examined. Further research is required to gain a deeper understanding into how the Wnt/β-catenin and NF-κB signaling pathways interact in UC. Such insights could ultimately contribute to the development of more effective therapeutic interventions for the treatment of UC.

PPAR-γ serves a crucial role in regulating lipid and glucose metabolism, as well as inflammatory responses (42,43). Notably, in patients with UC, there is a negative association between PPAR-γ expression and disease severity (44). By activating PPAR-γ, inflammatory factors can be inhibited to reduce the inflammatory response in the colonic mucosa, thereby improving the condition of patients with UC (45). On the other hand, a previous study reported that PPAR-γ functions as a brake on the Wnt/β-catenin signaling pathway (46). Consequently, the activation of PPAR-γ effectively inhibits the Wnt/β-catenin signaling pathway (47). Whether downregulation of the Wnt/β-catenin signaling pathway also leads to the activation of the PPAR-γ signaling pathway remains to be investigated. However, the present study demonstrated that XAV939 treatment did not increase the expression levels of PPAR-γ, suggesting that PPAR-γ potentially resides upstream of β-catenin. This finding underscores the importance of PPAR-γ as a potential therapeutic target in modulating both inflammatory processes and the Wnt/β-catenin signaling cascade in UC. Further exploration of the intricate interplay between these pathways and their respective regulators may reveal novel strategies for the management of symptoms and progression of UC.

Within the intestinal tract, enterocytes serve as a vital barrier, as they are responsible for nutrient absorption and defense against harmful microbial invasion (48). A number of studies have reported that UC is associated with the

loss of colonic crypt structures, and disruption of enterocytes impacts intestinal absorption and compromises the barrier function of the intestine (49,50). Through the use of single-cell sequencing, research has shown a notable decrease in the population of enterocytes and their progenitor cells within the intestines of patients with UC (51). Villin serves as a marker for enterocytes, and the present *in vivo* and *in vitro* experiments demonstrated that XAV939 could not reverse the differentiation of enterocytes. Notably, the differentiation of enterocytes is regulated by both the Wnt/β-catenin signaling pathway and the Notch signaling pathway. XAV939 cannot promote the differentiation of enterocytes by inhibiting Wnt/β-catenin alone (52). The present results demonstrated an association between PPAR-γ and Villin expression, implying that PPAR-γ may serve a regulatory role in the differentiation of enterocytes. A study examining the fruit fly intestine showed that the activation of the PPAR-γ homolog, ecdysone-induced protein 75B, stimulated the differentiation of ISCs into absorptive intestinal epithelial cell lineages (53). Furthermore, it has been documented that the UC risk gene, organic cation/carnitine transporter 2 (OCTN2), is under the regulatory influence of PPAR-γ, and that OCTN2 is predominantly expressed in enterocytes (54-56). OCTN2 participates in the transport of carnitine, which is a crucial step in fatty acid oxidation (FAO). Repairing the impeded FAO improved ISC function and ameliorated DSS-induced colitis in mice (57). Research has shown that improving oxidative phosphorylation metabolism enhanced mitochondrial function in intestinal epithelial cells and reduced DSS-induced intestinal inflammation (58). Thereby, continuous and in-depth research on the dysregulation of energy metabolism in enterocytes, as well as the regulatory role of PPAR-γ, may offer valuable insights into the underlying mechanisms of UC.

The results of the present *in vivo* experiments on the effects of XAV939 on PPAR-γ and Villin were inconsistent with those obtained from intestinal organoid cultures. The potential reasons include the effect of microenvironment and the impact of Wnt/β-catenin signaling on ISCs expansion. In the crypt, the ISCs are protected by surrounding niche cells (59). However, under *ex vivo* conditions, ISCs are directly exposed to the XAV939. The activation of the Wnt/β-catenin signaling pathway *ex vivo* mainly originates from Wnt ligands and enhancers in the culture medium, while Wnt signals in the crypt mainly come from niche cells, which are more stable (60). Additionally, a certain level of Wnt signaling is necessary for the maintenance and expansion of ISCs. The loss of other sources of Wnt activation *ex vivo* hinders the expansion of stem cells, which partly explained why XAV939 intervention *ex vivo* led to a further decrease in PPAR-γ and Villin expression.

In conclusion, the present study showed that XAV939 did not improve inflammation or intestinal morphology in DSS-induced UC. However, the present study elucidated the role of XAV939 in regulating ISC for DSS-induced intestinal injury through inhibition of the Wnt/β-catenin pathway (Fig. 7). Considering the significance of PPAR-γ and the differentiation of enterocytes, it is necessary to further investigate their interaction and understand the underlying mechanisms. Furthermore, given the complexity of UC and the involvement of multiple inflammatory pathways, a single agent such as XAV939 may not be sufficient to address all aspects of the disease. Consequently, a combination of therapeutic strategies targeting different inflammatory pathways and ISC functions may be necessary for effective UC treatment.

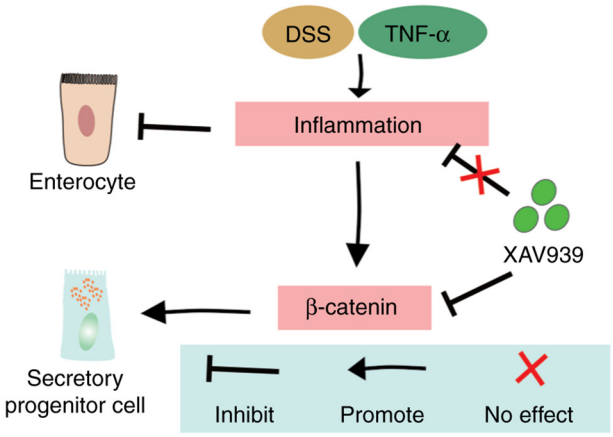

Figure 7. Schematic of the effects of XAV939 effects on intestinal stem cell differentiation alterations caused by inflammation. XAV939 reduced the number of secretory cell progenitor cells by inhibiting the Wnt/β-catenin signaling pathway but did not increase the number of enterocytes. DSS, dextran sulfate sodium.

Acknowledgements

Not applicable.

Funding

This work was supported by the Guangdong Basic and Applied Basic Research Foundation (grant no. 2023A1515110203) and the Postdoctoral Startup Fund of Shunde Women and Children's Hospital of Guangdong Medical University (grant no. 2022BSHQD002).

Availability of data and materials

The data generated in the present study may be found in the Gene Expression Omnibus database under accession number GSE275191 or at the following URL: https://www.ncbi.nlm.nih.gov/geo/query/acc.cgi?acc=GSE275191.

Authors' contributions

LWX and DJZ conceived the research and critically revised the manuscript. SJL, DBM and KW performed the experiments and prepared the manuscript. SJL and KW confirm the authenticity of all the raw data. All authors read and approved the final version of the manuscript.

Ethics approval and consent to participate

All animal procedures were performed in accordance with the Guidelines for Care and Use of Laboratory Animals of Guangdong Medical University and experiments were approved by Ethics Committee of Shunde Maternal and

Children's Hospital of Guangdong Medical University (approval no. 2023054).

Patient consent for publication

Not applicable.

Competing interests

The authors declare that they have no competing interests.

Reference

1. Le Berre C, Honap S and Peyrin-Biroulet L: Ulcerative colitis. Lancet 402: 571-584, 2023.
2. Wang M, Fu R, Xu D, Chen Y, Yue S, Zhang S and Tang Y: Traditional Chinese Medicine: A promising strategy to regulate the imbalance of bacterial flora, impaired intestinal barrier and immune function attributed to ulcerative colitis through intestinal microecology. J Ethnopharmacol 318: 116879, 2024.
3. Hassan SA, Kapur N, Sheikh F, Fahad A and Jamal S: Disease clearance in ulcerative colitis: A new therapeutic target for the future. World J Gastroenterol 30: 1801-1809, 2024.
4. Le Berre C, Roda G, Nedeljkovic Protic M, Danese S and Peyrin-Biroulet L: Modern use of 5-aminosalicylic acid compounds for ulcerative colitis. Expert Opin Biol Ther 20: 363-378, 2020.
5. De Deo D, Dal Buono A, Gabbiadini R, Spaggiari P, Busacca A, Masoni B, Ferretti S, Bezzio C and Armuzzi A: Management of proctitis in ulcerative colitis and the place of biological therapies. Expert Opin Biol Ther 24: 443-453, 2024.
6. Heimann TM, Swaminathan S, Slater GI and Kurtz RJ: Perianal fistula after ileoanal pouch in patients with ulcerative colitis: A review of 475 patients operated on at a major IBD center. Dis Colon Rectum 65: 76-82, 2022.
7. Hou Q, Huang J, Ayansola H, Masatoshi H and Zhang B: Intestinal stem cells and immune cell relationships: Potential therapeutic targets for inflammatory bowel diseases. Front Immunol 11: 623691, 2021.
8. Quandt J, Arnovitz S, Haghi L, Woehlk J, Mohsin A, Okoreeh M, Mathur PS, Emmanuel AO, Osman A, Krishnan M, *et al*: Wnt-β-catenin activation epigenetically reprograms T_{reg} cells in inflammatory bowel disease and dysplastic progression. Nat Immunol 22: 471-484, 2021.
9. Swafford D, Shanmugam A, Ranganathan P, Manoharan I, Hussein MS, Patel N, Sifuentes H, Koni PA, Prasad PD, Thangaraju M and Manicassamy S: The Wnt-β-catenin-IL-10 signaling axis in intestinal APCs protects mice from colitis-associated colon cancer in response to gut microbiota. J Immunol 205: 2265-2275, 2020.
10. Chang M, Chang L, Chang HM and Chang F: Intestinal and extraintestinal cancers associated with inflammatory bowel disease. Clin Colorectal Cancer 17: e29-e37, 2018.
11. Hirano T, Hirayama D, Wagatsuma K, Yamakawa T, Yokoyama Y and Nakase H: Immunological mechanisms in inflammation-associated colon carcinogenesis. Int J Mol Sci 21: 3062, 2020.
12. Li F, Yan H, Jiang L, Zhao J, Lei X and Ming J: Cherry polyphenol extract ameliorated dextran sodium sulfate-induced ulcerative colitis in mice by suppressing Wnt/β-catenin signaling pathway. Foods 11: 49, 2021.
13. Dong LN, Wang M, Guo J and Wang JP: Influences of probiotics combined with sulfasalazine on rats with ulcerative colitis via the Wnt/β-catenin signaling pathway. Eur Rev Med Pharmacol Sci 23: 6371-6378, 2019.
14. Jang J, Jung Y, Chae S, Bae T, Kim SM, Shim YJ, Chung SI and Yoon Y: XAV939, a Wnt/β-catenin pathway modulator, has inhibitory effects on LPS-induced inflammatory response. Immunopharmacol Immunotoxicol 41: 394-402, 2019.
15. Yao YY, Bian LG, Yang P, Sui Y, Li R, Chen YL, Sun L, Ai QL, Zhong LM and Lu D: Gastrodin attenuates proliferation and inflammatory responses in activated microglia through Wnt/β-catenin signaling pathway. Brain Res 1717: 190-203, 2019.
16. Takahashi T: Roles of nAChR and Wnt signaling in intestinal stem cell function and inflammation. Int Immunopharmacol 81: 106260, 2020.
17. Hiramatsu Y, Fukuda A, Ogawa S, Goto N, Ikuta K, Tsuda M, Matsumoto Y, Kimura Y, Yoshioka T, Takada Y, *et al*: Arid1a is essential for intestinal stem cells through Sox9 regulation. Proc Natl Acad Sci USA 116: 1704-1713, 2019.
18. Moparthi L and Koch S: Wnt signaling in intestinal inflammation. Differentiation 108: 24-32, 2019.
19. Parikh K, Antanaviciute A, Fawkner-Corbett D, Jagielowicz M, Aulicino A, Lagerholm C, Davis S, Kinchen J, Chen HH, Alham NK, *et al*: Colonic epithelial cell diversity in health and inflammatory bowel disease. Nature 567: 49-55, 2019.
20. Wei P, He Q, Liu T, Zhang J, Shi K, Zhang J and Liu S: Baitouweng decoction alleviates dextran sulfate sodium-induced ulcerative colitis by suppressing leucine-related mTORC1 signaling and reducing oxidative stress. J Ethnopharmacol 304: 116095, 2023.
21. Zhang H, Lang W, Li S, Xu C, Wang X, Li Y, Zhang Z, Wu T and Feng M: Corynoline ameliorates dextran sulfate sodium-induced colitis in mice by modulating Nrf2/NF-κB pathway. Immunopharmacol Immunotoxicol 45: 26-34, 2023.
22. Distler A, Deloch L, Huang J, Dees C, Lin NY, Palumbo-Zerr K, Beyer C, Weidemann A, Distler O, Schett G and Distler JH: Inactivation of tankyrases reduces experimental fibrosis by inhibiting canonical Wnt signalling. Ann Rheum Dis 72: 1575-1580, 2013.
23. Anders S, Pyl PT and Huber W: HTSeq-a Python framework to work with high-throughput sequencing data. Bioinformatics 31: 166-169, 2015.
24. Lachmann A, Clarke DJB, Torre D, Xie Z and Ma'ayan A: Interoperable RNA-Seq analysis in the cloud. Biochim Biophys Acta Gene Regul Mech 1863: 194521, 2020.
25. Robinson MD, McCarthy DJ and Smyth GK: edgeR: a Bioconductor package for differential expression analysis of digital gene expression data. Bioinformatics 26: 139-140, 2010.
26. McDermaid A, Monier B, Zhao J, Liu B and Ma Q: Interpretation of differential gene expression results of RNA-seq data: Review and integration. Brief Bioinform 20: 2044-2054, 2019.
27. Mi JX, Zhang YN, Lai Z, Li W, Zhou L and Zhong F: Principal component analysis based on nuclear norm minimization. Neural Netw 118: 1-16, 2019.
28. Yoo YE, Lee S, Kim W, Kim H, Chung C, Ha S, Park J, Chung Y, Kang H and Kim E: Early chronic memantine treatment-induced transcriptomic changes in wild-type and Shank2-mutant mice. Front Mol Neurosci 14: 712576, 2021.
29. Livak KJ and Schmittgen TD: Analysis of relative gene expression data using real-time quantitative PCR and the 2(-Delta Delta C(T)) method. Methods 25: 402-408, 2001.
30. Liang B, Jiang Y, Song S, Jing W, Yang H, Zhao L, Chen Y, Tang Q, Li X, Zhang L, *et al*: ASPP2 suppresses tumour growth and stemness characteristics in HCC by inhibiting Warburg effect via WNT/β-catenin/HK2 axis. J Cell Mol Med 27: 659-671, 2023.
31. Ming Z, Vining B, Bagheri-Fam S and Harley V: SOX9 in organogenesis: Shared and unique transcriptional functions. Cell Mol Life Sci 79: 522, 2022.
32. Kitamura S, Miyazaki Y, Shinomura Y, Kondo S, Kanayama S and Matsuzawa Y: Peroxisome proliferator-activated receptor gamma induces growth arrest and differentiation markers of human colon cancer cells. Jpn J Cancer Res 90: 75-80, 1999.
33. Centonze M, Berenschot EJW, Serrati S, Susarrey-Arce A and Krol S: The fast track for intestinal tumor cell differentiation and in vitro intestinal models by inorganic topographic surfaces. Pharmaceutics 14: 218, 2022.
34. Yang C and Merlin D: Unveiling colitis: A journey through the dextran sodium sulfate-induced model. Inflamm Bowel Dis 30: 844-853, 2024.
35. Zhong Y, Wang K, Zhang Y, Yin Q, Li S, Wang J, Zhang X, Han H and Yao K: Ocular Wnt/β-catenin pathway inhibitor XAV939-loaded liposomes for treating alkali-burned corneal wound and neovascularization. Front Bioeng Biotechnol 9: 753879, 2021.
36. Liu J, Kang R and Tang D: Lipopolysaccharide delivery systems in innate immunity. Trends Immunol 45: 274-287, 2024.
37. So T and Ishii N: The TNF-TNFR family of co-signal molecules. Adv Exp Med Biol 1189: 53-84, 2019.
38. Shi J, Ma C, Hao X, Luo H and Li M: Reserve of Wnt/β-catenin signaling alleviates mycoplasma pneumoniae P1-C-induced Inflammation in airway epithelial cells and lungs of mice. Mol Immunol 153: 60-74, 2023.
39. Chen T, Zhou R, Chen Y, Fu W, Wei X, Ma G, Hu W and Lu C: Curcumin ameliorates IL-1β-induced apoptosis by activating autophagy and inhibiting the NF-κB signaling pathway in rat primary articular chondrocytes. Cell Biol Int 45: 976-988, 2021.

40. Zhou J, Wu H, Hou J, Wang J, Wang J, Li M, Yao X, Gao J and Zhang Q: Daurisoline alleviated experimental colitis in vivo and in vitro: Involvement of NF-κB and Wnt/β-catenin pathway. Int Immunopharmacol 108: 108714, 2022.
41. Ma B and Hottiger MO: Crosstalk between Wnt/β-catenin and NF-κB signaling pathway during inflammation. Front Immunol 7: 378, 2016.
42. Caioni G, Viscido A, d'Angelo M, Panella G, Castelli V, Merola C, Frieri G, Latella G, Cimini A and Benedetti E: Inflammatory bowel disease: New insights into the interplay between environmental factors and PPARγ. Int J Mol Sci 22: 985, 2021.
43. Wang N, Kong R, Han W, Bao W, Shi Y, Ye L and Lu J: Honokiol alleviates ulcerative colitis by targeting PPAR-γ-TLR4-NF-κB signaling and suppressing gasdermin-D-mediated pyroptosis in vivo and in vitro. Int Immunopharmacol 111: 109058, 2022.
44. Fang J, Wang H, Xue Z, Cheng Y and Zhang X: PPARγ: The central mucus barrier coordinator in ulcerative colitis. Inflamm Bowel Dis 27: 732-741, 2021.
45. Venkataraman B, Ojha S, Belur PD, Bhongade B, Raj V, Collin PD, Adrian TE and Subramanya SB: Phytochemical drug candidates for the modulation of peroxisome proliferator-activated receptor γ in inflammatory bowel diseases. Phytother Res 34: 1530-1549, 2020.
46. Selim MA, Mosaad SM and El-Sayed NM: Lycopene protects against Bisphenol A induced toxicity on the submandibular salivary glands via the upregulation of PPAR-γ and modulation of Wnt/β-catenin signaling. Int Immunopharmacol 112: 109293, 2022.
47. Jeon KI, Phipps RP, Sime PJ and Huxlin KR: Antifibrotic actions of peroxisome proliferator-activated receptor γ ligands in corneal fibroblasts are mediated by β-catenin-regulated pathways. Am J Pathol 187: 1660-1669, 2017.
48. Oda M, Hatano Y and Sato T: Intestinal epithelial organoids: Regeneration and maintenance of the intestinal epithelium. Curr Opin Genet Dev 76: 101977, 2022.
49. Dunleavy KA, Raffals LE and Camilleri M: Intestinal barrier dysfunction in inflammatory bowel disease: Underpinning pathogenesis and therapeutics. Dig Dis Sci 68: 4306-4320, 2023.
50. Rath T, Atreya R and Neurath MF: A spotlight on intestinal permeability and inflammatory bowel diseases. Expert Rev Gastroenterol Hepatol 17: 893-902, 2023.
51. Li G, Zhang B, Hao J, Chu X, Wiestler M, Cornberg M, Xu CJ, Liu X and Li Y: Identification of novel population-specific cell subsets in chinese ulcerative colitis patients using single-cell RNA sequencing. Cell Mol Gastroenterol Hepatol 12: 99-117, 2021.
52. Liang SJ, Li XG and Wang XQ: Notch signaling in mammalian intestinal stem cells: Determining cell fate and maintaining homeostasis. Curr Stem Cell Res Ther 14: 583-590, 2019.
53. Zipper L, Jassmann D, Burgmer S, Görlich B and Reiff T: Ecdysone steroid hormone remote controls intestinal stem cell fate decisions via the PPARγ-homolog Eip75B in Drosophila. Elife 9: e55795, 2020.
54. Kong L, Pokatayev V, Lefkovith A, Carter GT, Creasey EA, Krishna C, Subramanian S, Kochar B, Ashenberg O, Lau H, *et al*: The landscape of immune dysregulation in Crohn's disease revealed through single-cell transcriptomic profiling in the ileum and colon. Immunity 56: 444-458.e5, 2023.
55. Smillie CS, Biton M, Ordovas-Montanes J, Sullivan KM, Burgin G, Graham DB, Herbst RH, Rogel N, Slyper M, Waldman J, *et al*: Intra- and inter-cellular rewiring of the human colon during ulcerative colitis. Cell 178: 714-730.e22, 2019.
56. Zhou S and Shu Y: Transcriptional regulation of solute carrier (SLC). Drug transporters. Drug Metab Dispos 50: 1238-1250, 2022.
57. Chen L, Jiao T, Liu W, Luo Y, Wang J, Guo X, Tong X, Lin Z, Sun C, Wang K, *et al*: Hepatic cytochrome P450 8B1 and cholic acid potentiate intestinal epithelial injury in colitis by suppressing intestinal stem cell renewal. Cell Stem Cell 29: 1366-1381.e9, 2022.
58. Kapur N, Alam MA, Hassan SA, Patel PH, Wempe LA, Bhogoju S, Goretsky T, Kim JH, Herzog J, Ge Y, *et al*: Enhanced mucosal mitochondrial function corrects dysbiosis and OXPHOS metabolism in IBD. bioRxiv [Preprint]: 2024.03.14.584471, 2024.
59. Yin X, Farin HF, van Es JH, Clevers H, Langer R and Karp JM: Niche-independent high-purity cultures of Lgr5+ intestinal stem cells and their progeny. Nat Methods 11: 106-112, 2014.
60. Hageman JH, Heinz MC, Kretzschmar K, van der Vaart J, Clevers H and Snippert HJG: Intestinal regeneration: Regulation by the microenvironment. Dev Cell 54: 435-446, 2020.